Characteristics and degradation of organic aerosols from cooking sources based on hourly observation of organic molecular markers in urban environment

Rui Li [a, b#], Kun Zhang [a, b#], Qing Li [a, b], Liumei Yang [a, b], Shunyao Wang [a, b], Zhiqiang Liu [a, b, c], Xiaojuan Zhang [a, b, c], Hui Chen [a, b], Yanan Yi [a, b], Jialiang Feng [a, b], Qiongqiong Wang [d], Ling Huang [a, b], Wu Wang [a, b], Yangjun Wang [a, b], Jian Zhen Yu [e, f], Li Li [a, b*]

[a] School of Environmental and Chemical Engineering, Shanghai University, Shanghai, China

[b] Key Laboratory of Organic Compound Pollution Control Engineering (MOE), Shanghai University, Shanghai, China

[c] Jiangsu Changhuan Environment Technology Co., Ltd., Changzhou, Jiangsu, China

[d] School of Environmental Studies, China University of Geosciences, Wuhan, 430074, China

[e] Department of Chemistry, Hong Kong University of Science & Technology, Hong Kong, China

[f] Division of Environment & Sustainability, Hong Kong University of Science & Technology, Hong Kong, China

# These two authors contributed equally to this work.

** Correspondence: Li Li (Lily@shu.edu.cn)*

Abstract

Molecular markers in organic aerosol (OA) provide specific source information of $PM_{2.5}$, and the contribution of cooking organic aerosols to OA is significant, especially in urban environments. However, the low time resolution of offline measurements limits the effectiveness in interpreting the tracer data, the diurnal variation of cooking emission and the oxidation process. In this study, we used on-line thermal desorption aerosol gas chromatography mass spectrometry (TAG) to measure organic molecular markers in fine particulate matter ($PM_{2.5}$) at an urban site in Changzhou, China. The concentrations of saturated fatty acids (sFA), unsaturated fatty acids (uFAs), and oxidative decomposition products of unsaturated fatty acids (ODPs) were measured every two hours to investigate the temporal variations and the oxidative decomposition characteristics of uFAs in urban environment. The average concentration of total fatty acids (TFAs, sum of sFAs and uFAs) was measured to be 105.7± 230.3 ng/m^3. The average concentration of TFAs in polluted period ($PM_{2.5}$ >

35 $\mu g/m^3$) was 147.1 ng/m^3, which was 4.2 times higher than that in clean period ($PM_{2.5}$ < 35 $\mu g/m^3$), higher than the enhancement of $PM_{2.5}$ (2.2 times) and organic carbon (OC) (2.0 times) concentrations comparing polluted period to clean period. The mean concentration of cooking aerosol in the polluted period (3.63 $\mu g/m^3$) was about 3.9 times higher than that in the clean period (0.90 $\mu g/m^3$), which was similar to the trend of fatty acids. Fatty acids showed a clear diurnal variation. Linoleic acid /stearic acid and oleic acid / stearic acid ratios were significantly higher at dinner time, and closer to the cooking source profile. By performing backward trajectory clustering analysis, under the influence of short-distance air masses from surrounding areas, the concentrations of TFAs and $PM_{2.5}$ were relatively high; while under the influence of air masses from easterly coastal areas, the oxidation degree of uFAs emitted from local culinary sources were higher. The effective rate constants (k_O) for the oxidative degradation of oleic acid were estimated to be 0.08-0.57 h^{-1}, which were lower than k_L (the estimated effective rate constants of linoleic acid, 0.16-0.80 h^{-1}). Both k_O and k_L showed a significant positive correlation with O_3, indicating that O_3 was the main night-time oxidants for uFAs in the Changzhou City. Using fatty acids as tracers, cooking was estimated to contribute an average of 4.6% to $PM_{2.5}$ concentrations, increased to 7.8% at dinner time. Cooking was an important source to OC, contributing to 8.1%, higher than the contribution to $PM_{2.5}$. This study investigates the variation of the concentrations and oxidative degradation of fatty acids and corresponding oxidation products in ambient air, which can be a guide for the refinement of aerosol source apportionment, and provide scientific support for the development of cooking source control policies.

1. Introduction

Organic aerosol (OA) is an important component of fine particulate matter ($PM_{2.5}$), accounting for 20-90% of the total $PM_{2.5}$ mass (Kanakidou et al., 2005). Among different OA sources, restaurant fumes are relatively important (Huang et al., 2021). The contribution of cooking organic aerosols (COA) to OA is significant, especially in urban environments, where COA can contribute 11%-34% to total organic carbon (OC) and 3%-9% to $PM_{2.5}$ mass concentration, even higher than traffic-related hydrocarbon-based OA (Huang et al., 2021; Li et al., 2020). The presence of carcinogenic mutagens in restaurant fumes contains chemicals that can be harmful to human immune function (Huang et al., 2020). According to the 2018 global cancer statistics, lung cancer accounts for 24.1% of all cancer deaths in China and is the most common cause of cancer-related deaths in China. The risk of cancer is associated with cooking events (Zhang et al., 2017). In previous studies on the molecular tracers of cooking source based on filter membrane sampling, the time resolution usually varies from one day to several days, which cannot accurately capture the diurnal variations of pollutants emitted by the cooking source (Li et al., 2021). The thermal desorption aerosol gas chromatography−mass spectrometry (TAG) enables online

monitoring of organic molecular markers (Wang et al., 2020). By clarifying the characteristics of cooking emissions, quantifying the concentrations of pollutants emitted from cooking and its contribution to urban OA on the diurnal time scales, we build up data and process knowledge about cooking-sourced $PM_{2.5}$ pollution, which in turn help us evaluate the option of controlling cooking emissions in the overall pollution prevention for urban environments.

Processes such as emission rate, atmospheric dilution, and photochemical oxidation can affect aerosol composition measured at receptor sites (Fortenberry et al., 2019; Yee et al., 2018). Particulate organic matter can undergo heterogeneous oxidation by ozone, OH and NO_3 radicals (Wang et al., 2020). When using organic tracer data from filter analysis, variations in concentration due to degradation or secondary production were reported (Ringuet et al., 2012). These degradation and generation processes in the atmosphere are therefore worthy of our attention when using organic markers as source tracers. The mechanism and kinetics of ozonolysis of oleic acid and linoleic acid in the presence of oxidants such as NO_3, O_3 and OH radicals have been extensively studied in the laboratory studies (Vesna et al., 2009; Zahardis and Petrucci, 2007; Ziemann, 2005). The aging of POA markers under atmospheric conditions, however, is still far from being properly understood with few field observations performed in this topic compared to laboratory studies (Bertrand et al., 2018a; Bertrand et al., 2018b). The high timely-resolved observations would help to fill this gap.

Cooking is an important source contributor to $PM_{2.5}$, especially in urban environments. Cooking sources have recently received increasing attention, but they are largely an uncontrolled source of $PM_{2.5}$. Saturated fatty acids (sFAs) and unsaturated fatty acids (uFAs), such as palmitic, stearic, and oleic acids, are known molecular markers from cooking emissions, which are released primarily during cooking activities from the hydrolysis and thermal oxidation of cooking oils. Fatty acids and their derivatives are often used as tracers in the receptor model for the source apportionment of $PM_{2.5}$. It has been found that nonanoic acid, 9-oxononononanoic acid and azelaic acid are the main atmospheric oxidation products of oleic acid in the aerosol, while uFAs such as oleic and linoleic acids also react with other atmospheric oxidants, such as OH (Nah et al., 2014; Wang et al., 2020).

In this study, TAG was employed at an urban site in Changzhou, China, to investigate the variation of atmospheric cooking-related fatty acids with hourly resolution data (Ren et al., 2019). The aim of this study is to identify the contribution of cooking emissions to ambient $PM_{2.5}$ with hourly organic molecular data and to investigate the oxidative decomposition reactions of cooking-related uFAs in an urban area. Results of this study could provide valid basis and insights for the refinement of $PM_{2.5}$ source apportionment as well as atmospheric modelling.

2. Methodology

2.1 Field measurement

Gaseous pollutants, $PM_{2.5}$ and its main chemical constituents as well as organic markers were measured online at the Changzhou Environmental Monitoring Center of Jiangsu Province (CEMC) (31.76N, 119.96E) during January-March 2021, which is a representative urban site (Fig. 1). Detailed information on instruments can be found in Text S1 of the Supporting Information. The meteorological parameters and gas pollutant data were obtained from CEMC observations and publicly available datasets from the China Meteorological Data Network (available at http://data.cma.cn, last access: Aug 16, 2022).

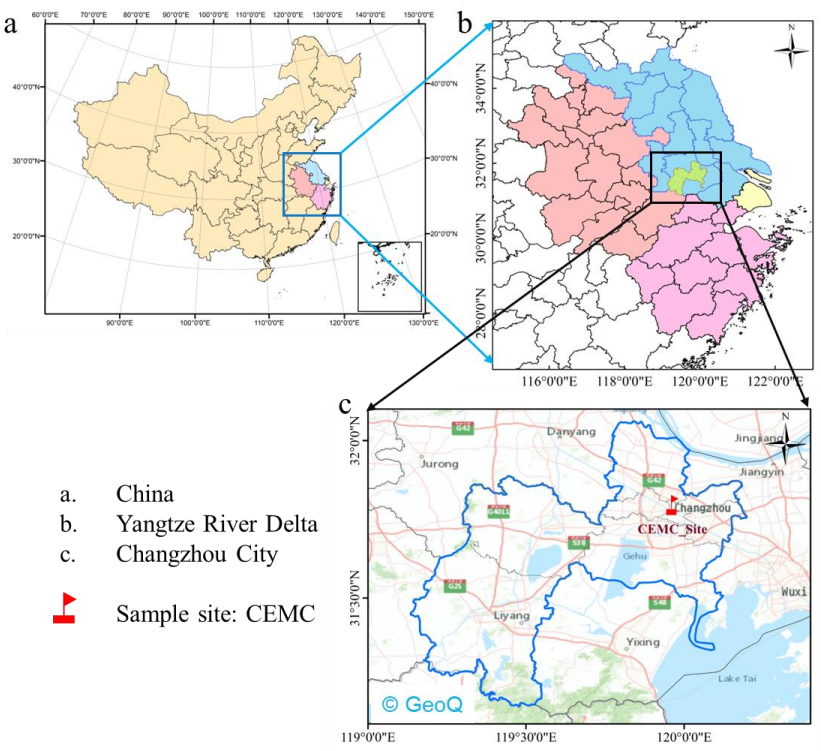

Figure 1. Location of the sampling site in Changzhou, China.

Quantification of hourly speciated organic markers was achieved using TAG. The operation details and data quality have been described in our previous work (Wang et al., 2020; Zhang et al., 2021). The sampling and analysis sequence of the TAG system includes four steps: (a) $PM_{2.5}$ sampling and synchronous gas chromatography-mass spectrometry (GC-MS) analysis of the previous sample; (b) loading of the internal standards (IS) from the standards (STD) reservoir to a thermal desorption cell; (c) derivatization and thermal desorption of analytes on the collection and thermal desorption (CTD) cell and subsequent preconcentration of the analytes in focusing trap (FT); and (d) loading of analytes into the GC column for GC-MS analysis. The following is a detailed description. Ambient air was sampled at a flow rate of 8.5-9.5

L/min through a cyclone with $PM_{2.5}$ cutting size (BGI Inc., Waltham, MA), a Nafion dryer (PERMA PURE, MD-700-24S-3) to remove moisture, and then through a carbon denuder (model: ADI-DEN2) to remove volatile organics. The sampled particles were collected on the CTD cell at 30°C for 60 min, followed by derivatization and thermal desorption for 8 min as the temperature of the CTD cell increases to 300°C in 2 min and maintains for 6 min, during which a 10 mL/min helium purge flow combined with a 40 mL/min derivatization flow with N-methyl- N-(trimethylsilyl) trifluoroacetamide (MSTFA) flow through for 8 min. Subsequently, the FT was heated to 300°C in 2 min and kept at 300°C for 10 min, transferring the analytes onto the GC column head (DB-5MS, size 30 m × 0.25 μm × 0.25 μm) by carrier gas. After GC separation, the target organics were sent to the MS detector for quantification. The GC-MS analysis duration for each sample was 60 min while collection of the next sample the CTD cell starts. With the current TAG instrumental set-up, samples were collected every even hour. The post-sampling steps, including in-situ derivatization, thermal desorption, GC-MS analysis, and standby step, took 2 h, thus producing 12 samples per day.

The summary of target organic molecular markers and internal standards (IS) are shown in Table 1. Identification of compounds was performed by comparing retention times and mass spectra with those of authentic standards (Vesna et al., 2009; Wang et al., 2020). Calibration curves were established by internal standard method. The correlation coefficients of the calibration curves range from 0.88-1.00. For compounds without authentic standards and for compounds whose authentic standards are not included in the current standard mixture, their identification is performed by comparing their mass spectra with the National Institute of Standards and Technology (NIST) libraries. Azelaic acid was identified and quantified by using authentic standards. Nonanoic acid and 9-oxononanoic acid were identified by comparison with mass spectra in the NIST library and by referring to Ziemann (2005), Pleik et al. (2016) and Wang et al. (2020). Ozone oxidation of oleic acid yields C_9 aldehydes and acids including nonanal, azelaic acid, nonanoic acid, and 9-oxononanoic acid. Since nonanal could also be primary in the gas phase, it is thus not discussed in this paper. The library of the NIST was identified and quantified using the alternative standards specified in Table 1.

Table 1. Statistics of hourly concentrations of organics associated with cooking emissions measured by TAG during the campaign.

Compounds	Average	Stdev	Min	Max	Quantification IS
Myristic acid [a]	0.69	1.33	0.03	10.14	Palmitic acid-d_{31}
Palmitic acid	38.77	84.14	1.45	670.12	Palmitic acid-d_{31}
Stearic acid	26.51	50.58	1.81	341.65	Palmitic acid-d_{31}
Oleic acid	32.15	81.34	0.96	723.95	Stearic acid-d_{35}
Linoleic acid [b]	7.80	28.32	0.09	326.50	Stearic acid-d_{35}
Nonanoic acid [c]	1.19	1.32	BD [d]	7.94	Adipic acid-d_{10}
9-oxononanoic acid [c]	3.91	4.73	0.19	17.18	Adipic acid-d_{10}
Azelaic acid	9.15	32.99	BD	309.64	Adipic acid-d_{10}

a, Quantified using palmitic acid as the surrogate; b, Quantified using oleic acid as the surrogate; c, Quantified using azelaic acid as the surrogate; d, Below detection limit.

2.2 Backward trajectory analysis

Backward trajectory analysis is a useful tool in identifying the influence of air masses on the chemical composition of $PM_{2.5}$ (Wang et al., 2017). Backward trajectories of 36-h duration arriving at an altitude of 100 m above ground level (AGL) over the CEMC site were calculated deploying the 0.5° Global Data Assimilation System (GDAS) meteorological data (https://www.ready.noaa.gov/archives.php, last access: Aug 16, 2022). The trajectories were then classified into different clusters according to the geographical origins and movement of the trajectories using the TrajStat model (Li et al., 2020).

2.3 Relative rate constant analysis

Ambient concentrations of species are influenced by its emissions, atmospheric dilution/compaction, chemical loss/production, and wet/dry deposition. As the target sFAs and uFAs in urban environments are predominately primary in their source origin, the chemical production rate could be assumed to be negligible. Donahue et al. (2005) formulated the relative rate expression for heterogeneous oxidation reactions of multicomponent OA. The specific expression applied to the ambient measurements of uFAs is derived, as given in Equation (Eq 1) and Equation (Eq 2) (Wang and Yu, 2021).

$$\frac{C_i}{C_s} = A \times e^{-kt} \quad (1)$$

$$k \approx k_{r_i} \times C_{OX} \quad (2)$$

C_i and C_s are the particle-phase concentration of species i and sFAs, respectively. Among the quantified sFA and uFA cooking markers, palmitic acid was selected as the reference molecule for normalization. Using the concentration ratio eliminates the interference from atmospheric dilution and deposition. Fitting the ambient C_i/C_s data versus t with an exponential function provides an estimate for k, the effective pseudo-first order decay rate (h^{-1}). k_{ri} is the second-order reaction rate constant of species i against an oxidant. C_{OX} is the average oxidant concentration in the aerosol.

2.4 Source apportionment based on PMF

Positive Matrix Factorization (PMF) is a bilinear factor analysis method, which is widely used to identify pollution sources and quantify their contributions to the ambient air pollutants at receptor sites, with an assumption of mass conservation between emission sources and receptors (Amato et al., 2009; Lee et al., 2008). In this study, the United States Environmental Protection Agency (USEPA) PMF version 5.0 (Norris et al., 2014) was applied to perform the analysis. PMF decomposes the measured data matrix, X_{ij}, into a factor profile matrix, f_{kj}, and a factor contribution matrix, g_{ik}, (Eq

3):

$$x_{ij} = \sum_{k=1}^{p} g_{ik} f_{kj} + e_{ij} \quad (3)$$

$$Q = \sum_{i=1}^{n} \sum_{j=1}^{m} (e_{ij}/u_{ij})^2 \quad (4)$$

where X_{ij} is the measured ambient concentration of target pollutants; g_{ik} is the source contribution of the k_{th} factor to the i_{th} sample, and f_{kj} is the factor profile of the j_{th} specie in the k_{th} factor; e_{ij} is the residual concentration for each data point. PMF seeks a solution that minimizes an object function Q (Eq 4), with the uncertainties of each observation (u_{ij}) provided by the user.

The uncertainty of each data point was calculated according to Eq 5:

$$u_{ij} = \sqrt{(x_{ij} \times EF)^2 + (\frac{1}{2} \times MDL)^2} \quad (5)$$

where MDL is the method detection limit and EF is the error fraction determined by the user and associated with the measurement uncertainties. The concentration data below MDL was replaced by 0.5 of the MDL, and the corresponding uncertainty u_{ij} was calculated by five-sixths of the MDL. Missing values were replaced by the median value of the species, and its u_{ij} was assigned as four times of the median value (Norris et al., 2014).

3. Results and discussion

The time series of hourly data of meteorological parameters, gaseous pollutants (including O_3 and NO_2), $PM_{2.5}$, water soluble ions (WSII), carbon components (Organic carbon, OC; Elemental carbon, EC) during the monitoring period (January 10-14, February 9-15 and March 11-16, 2021) are shown in Fig.2. During the campaign, the average temperature (T), relative humidity (RH) and wind speed (WS) was 10.9±4.5 ℃, 55.3±18.2% and 1.2±0.5 m/s, respectively. The average concentrations of gas pollutants, $PM_{2.5}$, WSII and OC/EC are listed in Table S1. The average concentrations of NO_2, O_3 and $PM_{2.5}$ were 42.85±25.89, 51.53±29.62 and 50.07±26.54 μg/m^3, respectively. Additionally, the average OC and EC concentrations were 6.57±4.63 and 2.12±2.04 μg/m^3 respectively, with the contribution of OC to $PM_{2.5}$ ranging from 4.7% to 26.8% (13.2% as average).

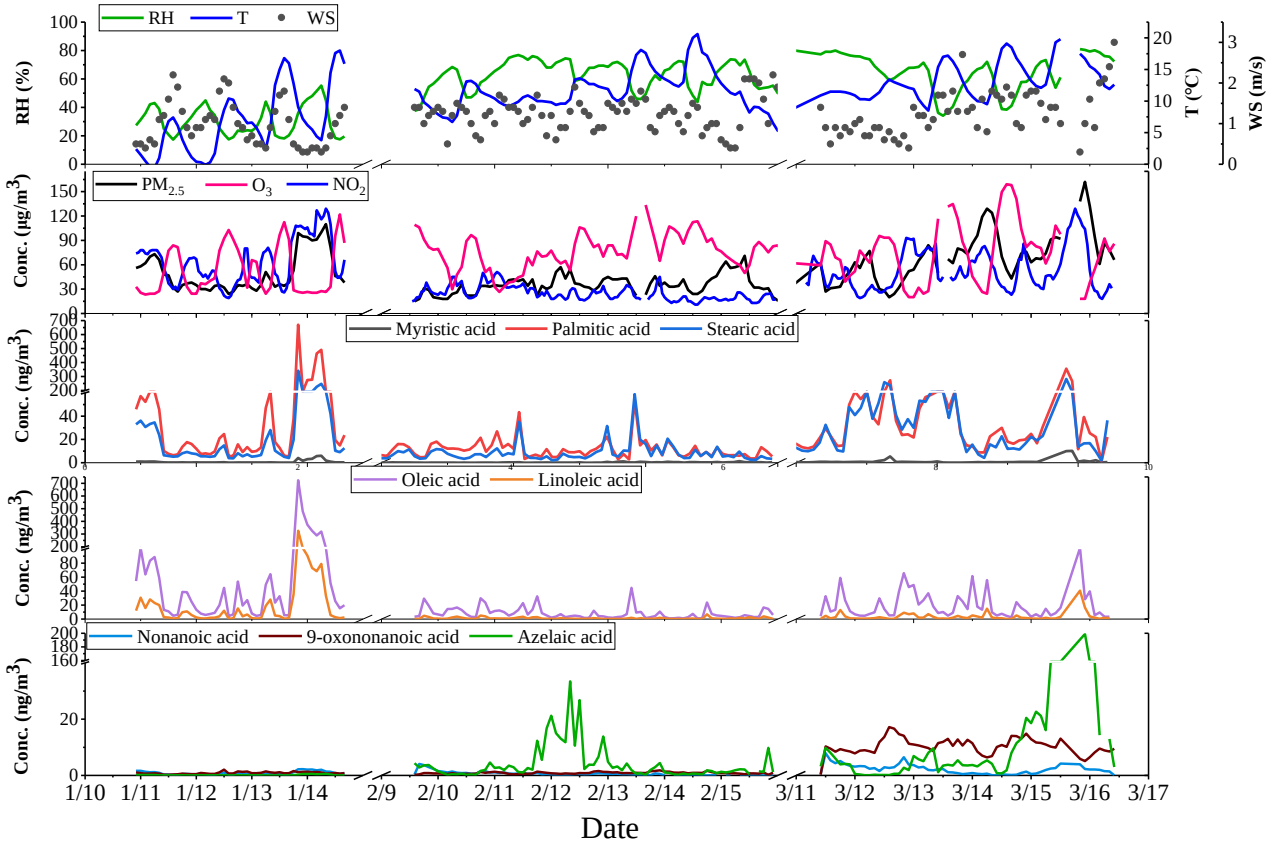

Figure 2. Time series of pollutants concentration and meteorological parameters

3.1 Characteristics of cooking-derived organic molecular markers

The fatty acids studied include three most abundant sFAs (myristic, palmitic and stearic acids) and two abundant uFAs (oleic and linoleic acids). The concentration of total fatty acids (TFAs, sum of the concentrations of the five fatty acids) was (105.70±230.28) ng/m^3, ranging from 8.30 to 2066.30 ng/m^3, which is close to the concentrations at the urban site in Shanghai (105 ng/m^3) (Li et al., 2020; Wang et al., 2020). The average percentage of TFAs in OC was 1.3% with the maximum value of 8.7% (The concentration of $PM_{2.5}$ at the corresponding time was 99 μg/m^3), which was 6.6 times higher than the average. It revealed that the composition of $PM_{2.5}$ could dramatically change, especially during the dinner time. The mean concentration of TFAs at dinner time was 160.71 ng/m^3, and the contribution of TFAs to $PM_{2.5}$ and OC mass concentration was 2.4‰ and 1.7%, respectively, which were 1.5 and 1.3 times of the mean during the observation period.

We define the "polluted period" as the periods with hourly $PM_{2.5}$ concentrations exceeding 35 μg/m^3, and the remaining periods are defined as "clean period". Table 2 shows the mean values of $PM_{2.5}$, OC and TFAs concentrations during the clean ($PM_{2.5}$ <35μg/m^3) and polluted periods. The mean concentration of $PM_{2.5}$ during the polluted period was 62.86 μg/m^3, which was 2.2 times higher than that during the clean period (28.29 μg/m^3). OC and $PM_{2.5}$ were similar, with concentrations during the pollution period being 2.0 times higher than during the clean period. The mean concentration of

TFAs in the polluted period was 147.06 ng/m^3, 4.2 times higher than that in the clean hour (35.28 ng/m^3). Additionally, the concentrations of sFAs and uFAs in the polluted hours were 4.3 and 4.1 times higher than those during the clean period, respectively.

The concentration of TFAs were influenced by emissions, accumulation, transport and dispersion of pollutants during the polluted periods (Hou et al., 2006; Schauer et al., 2003). The fatty acid content of 1.95 ng/μg in $PM_{2.5}$ during the polluted period was 2.7 times greater than that of 1.24 ng/μg during the clean period, which was smaller than the variation range of $PM_{2.5}$ and OC concentrations before and after the polluted period. The variation of TFAs in OC was similar to that in $PM_{2.5}$. The change in TFAs/OC was weaker than the change in OC, mainly because cooking has relatively small fluctuations in emissions, while the increase in OC concentration was more significant with simultaneous contributions from other sources (e.g., biomass burning, coal combustion, and vehicle exhaust). Similarly, the mass concentration of $PM_{2.5}$ was driven by emission source significantly. Table S1 shows the contribution of total fatty acids directly emitted from various sources to OC, in which the contribution of TFAs from vehicle exhaust is the least, and the proportion of TFAs emitted from cooking in OC is higher than that from other sources. The observed contribution of TFAs to OC in $PM_{2.5}$ was smaller than TFAs/OC ratio in cooking, but larger than that in other sources.

Table 2. $PM_{2.5}$ concentration, organic carbon fraction and fatty acids concentration during clean and polluted periods.

Species	Clean period	Polluted period	Polluted/clean
$PM_{2.5}$ (μg/m^3)	28.29	62.86	2.2
OC (μg/m^3)	4.05	8.00	2.0
TFAs (ng/m^3)	35.28	147.06	4.2
sFAs (ng/m^3)	21.60	92.05	4.3
uFAs (ng/m^3)	13.68	55.53	4.1
TFAs/$PM_{2.5}$ (ng/μg)	1.24	1.95	1.6
TFAs/OC (ng/μg)	16.84	22.61	1.3

Similar variation and diurnal patterns were found for these five fatty acids (Fig.3), confirming their common origin. In addition, compared to fatty acids, the time series of C_9 acids showed a different diurnal variation, suggesting different production and reaction processes. Fatty acids showed a clear diurnal variation, with two peaks observed at around 6:00 and 20:00 local time, respectively, and the dinner time peak was especially prominent. In contrast to the previous observations in Shanghai, no peak was observed at lunchtime. The relatively higher boundary layer during the daytime, facilitated the diffusion of pollutants. The weaker oxidation of uFAs emitted at night made the fatty acid concentration peaks more pronounced at dinner time (Wang et al., 2020). Figure 3(b) shows the contribution of various fatty acids to OC. When the influence of the boundary layer height change was eliminated, the proportion of the five fatty acids and TFAs in

OC at noon had a weaker peak, which was still smaller than that during the morning and evening mealtimes. In conclusion, the apparent peaks of TFAs at the dinner time provide strong evidence for source contribution to air pollution from local cooking emissions.

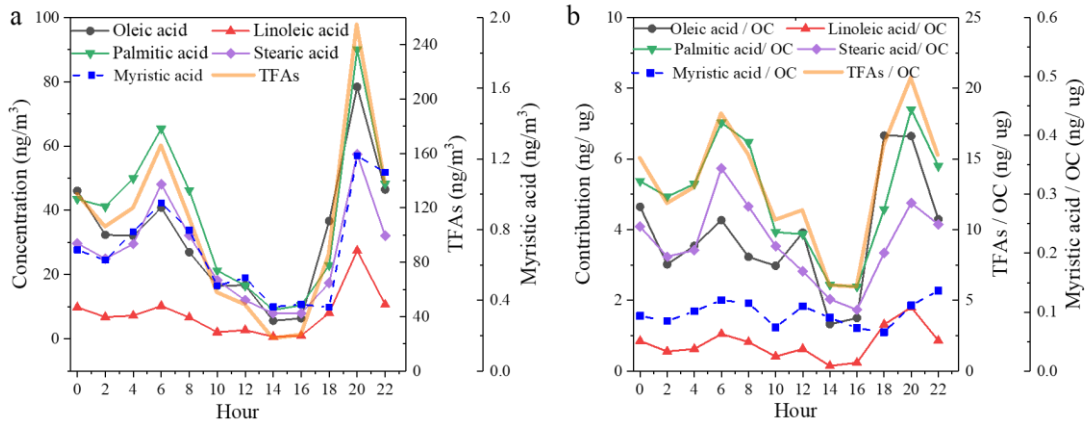

Figure 3. Diurnal variation of five fatty acids and TFAs during the observation period.

Fatty acids in urban atmospheres are influenced by various anthropogenic (e.g., biomass burning, vehicle exhaust) (Hays et al., 2002; Schauer et al., 2001; Simoneit, 2002; Wang et al., 2009) and biogenic sources (Oliveira et al., 2007; Rogge et al., 2006). The main sources of fatty acid-like substances in the atmospheric environment of the study area can be discerned on the basis of characteristic ratios between fatty acids emitted from different sources (Fig.4) (He et al., 2004; Pei et al., 2016; Rogge et al., 1993; Zhao et al., 2015; Zhao et al., 2007). The palmitic acid to stearic acid (P/S) ratios observed in this study had a range between 0.49 and 3.08 (average value: 1.49), significantly lower than those associated with residential coal combustion and industrial coal combustion, while partially overlapping those from biomass burning, vehicle exhaust and sea spray aerosol (Bikkin et al., 2019; Cai et al., 2017; Ho et al., 2015; Zhang et al., 2008; Zhang et al., 2007). Ho et al. (2015) studied urban areas in Beijing where fatty acid concentrations were elevated during traffic restrictions compared to non-restricted periods, suggesting that motor vehicle exhaust is not a significant source of fatty acids in urban areas. In the study of Simoneit (2002), no oleic acid was detected in organic molecular substances from biomass burning. The oleic acid/stearic acid (O/S) ratio from sea spray aerosol samples is 0.16 (Bikkin et al., 2019), which is obviously lower than the ambient data in this study (1.4). Thus, it is reasonable to conclude that biomass burning, vehicle exhaust and sea spray were insignificant sources of fatty acids in urban Changzhou during the observation in this study. Especially during the dinner period, when the O/S ratio was significantly higher and close to the ratio in the organics emitted from traditional culinary types in the Yangtze River Delta region.

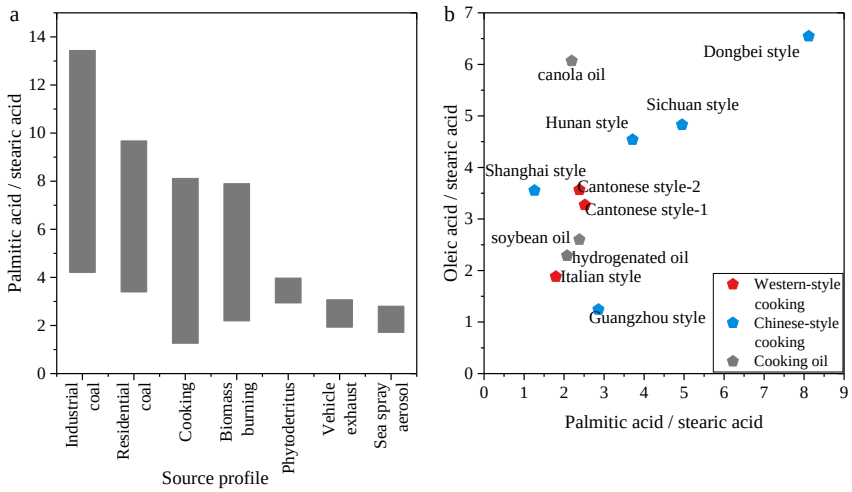

Figure 4. Ratio of fatty acids (P/S) in organic molecular substances emitted directly from different sources (a); Ratio of fatty acids (P/S vs O/S) emitted by different types of cooking sources (b).

Information on the changes of specific molecular markers is useful in investigating the aging process of aerosol. The two uFAs (oleic acid and linoleic acid) are more reactive with atmospheric oxidants (OH and O_3, etc.) in the atmosphere due to the presence of C=C bonds, compared to sFAs. Furthermore, the two homologous sFAs (palmitic and stearic acid) have similar chemical structures, reactivity and volatility, thus their concentration ratios can be assumed to remain constant during post-emission periods. Therefore, the ratio of P/S mainly depends on the sources. Fig.5 shows the O/S ratios and linoleic acid/ stearic acid (L/S) versus P/S, respectively. The average value of P/S was 1.49±0.49, which was within the range of cooking source profile values measured from direct emissions from different restaurants and cooking types (1.3-8.1) (He et al., 2004; Pei et al., 2016; Schauer et al., 2002; Zhao et al., 2007), and similar to the ratio of P/S in atmospheric $PM_{2.5}$ in Shanghai (1.9) (Li et al., 2020; Wang et al., 2020). In this study, the O/S ratio (1.4 ± 1.1) of the ambient samples was overall in the range of the cooking source profile (1.2-6.5, with an average of 3.6), while the L/S ratio of 0.25 ± 0.31 was slightly lower than the cooking source profile values (1.1-5.8, and the average was 2.9) (He et al., 2004; Pei et al., 2016; Schauer et al., 2002; Zhao et al., 2007), indicating that linoleic acid is more easily degraded than oleic acid. The O/S ratio of the ambient samples in this study was higher than those measured in Beijing (0.65) (He et al., 2004) from January to October and in Shanghai (0.83) (Li et al., 2020; Wang et al., 2020) during winter.

The diurnal variations of O/S and L/S are also shown in Fig.5. The ratios were significantly higher during dinner time (18:00-20:00), and were closer to the cooking source profile. Demonstrating that fresh emissions entered into the atmosphere during cooking period, especially dinner time, while uFAs were quickly consumed during aging. The ratio of linoleic acid to stearic acid is consistently lower than what is involved in the source spectrum, which may be influenced by different regions and source characteristics from different types of restaurants.

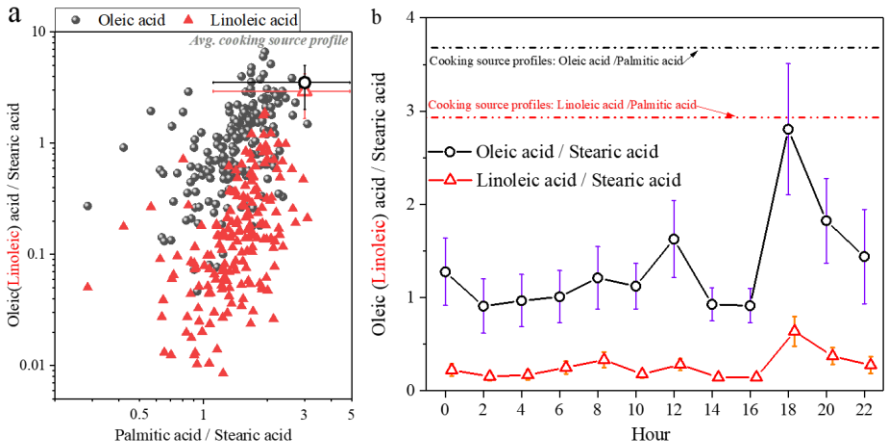

Figure 5. The oleic/ stearic acid and linoleic/ stearic acid ratios compared to the palmitic/stearic acid ratio (a); diurnal variation in the ratio of oleic (linoleic) acid to stearic acid concentration (b). (The cooking source profile values were measured from direct emissions from different restaurants and cooking types.)

3.2 Backward trajectory clustering analysis

The best solution of four clusters was determined based on the variation of the total spatial variance (Fig.6 and Figure S2). Fig.7 shows the four cluster solutions and the mean distribution of meteorological conditions and pollutants in each cluster. Briefly, cluster #1 (CL#1), which represents 15.4% of the sample, comes from the northwest continental region of China and reaches Changzhou before passing Gansu, Shan'xi and Henan provinces, and the lower temperature and humidity associated with this cluster are consistent with its geographic origin. Cluster #2 (CL#2), which accounts for 35.6% of the total number of trajectories, represents air masses from the northeastern part of the ocean, and the temperature and humidity associated with this cluster are higher than those of CL#1. Cluster 3 (CL#3), contributing 18.6%, traveling slowly from inland area, is associated with the lowest wind speed, with higher temperature and humidity than CL#1 but lower than CL#2. Cluster 4 (CL#4), representing 30.3% of the trajectories, represents the eastern/southeastern oceanic air masses, with the highest observed temperature, humidity and wind speed among all of the air masses. CL#2 and CL#4 have relatively high temperature, humidity and wind speed. CL#3 is associated with the highest NO_2 concentrations, confirming its local air mass origin, and the $PM_{2.5}$ and OC concentrations in this air mass are also the highest compared to all the other air masses.

The concentrations of sFAs, uFAs and their oxidation products under each cluster are shown in Fig.5. The total concentrations of sFAs, uFAs and uFAs' oxidative decomposition products (ODPs, in this study, ODPs includes azelaic acid, nonanoic acid and 9-oxononononanoic acid) within the four types of air mass clusters were in the order of CL#3>CL#2>CL#4>CL#1, where the TFAs in CL#1 and CL#3 were larger than the percentages in CL#2 and CL#4. The relative contents of sFAs and uFAs in CL#1 and CL#3 are closer than those in the other two types of air masses, and are

closer to the concentration ratio of the species directly emitted from the cooking source (the value of uFAs /sFAs range from 0.8 to 3.2) (He et al., 2004; Pei et al., 2016; Schauer et al., 2002; Zhao et al., 2007), which indicated that the oxidative decomposition of uFAs is less in CL#1 and CL#3. CL#3 was a slowly moving, local cluster. Under this air mass clustering, local emissions contribute significantly to fatty acids as well as $PM_{2.5}$ concentration. The air mass of CL#1 exhibits the longest range, the concentrations of ODPs were relatively small among all air masses, and the low ODPs concentration was inconsistent with other literature findings of more aging aerosol production from long-range transport (Wang et al., 2020). The lowest $PM_{2.5}$ concentrations and cleaner air masses during air mass CL#1 suggested that long-range air mass transport from the northwest was not the main source of fatty acids and ODPs in Changzhou during the observation. The value of uFAs /sFAs in CL#2 and CL#4 was less than that in CL#1 and CL#3 and less than the ratio in sources. In addition, the proportion of ODPs in CL#2 and CL#4 is greater than that in CL#1 and CL#3. This result may be explained by the following two reasons: first, under the influence of transport, the air masses brought more sFAs, ODPs, and the air masses were more aged; second, under the influence of CL#2 and CL#4 air masses, in which the ozone concentration was higher than other air masses, the decomposition reaction of uFAs was more active and could produce more ODPs. In addition, the oxidative reaction of uFAs could be influenced by meteorological conditions as well.

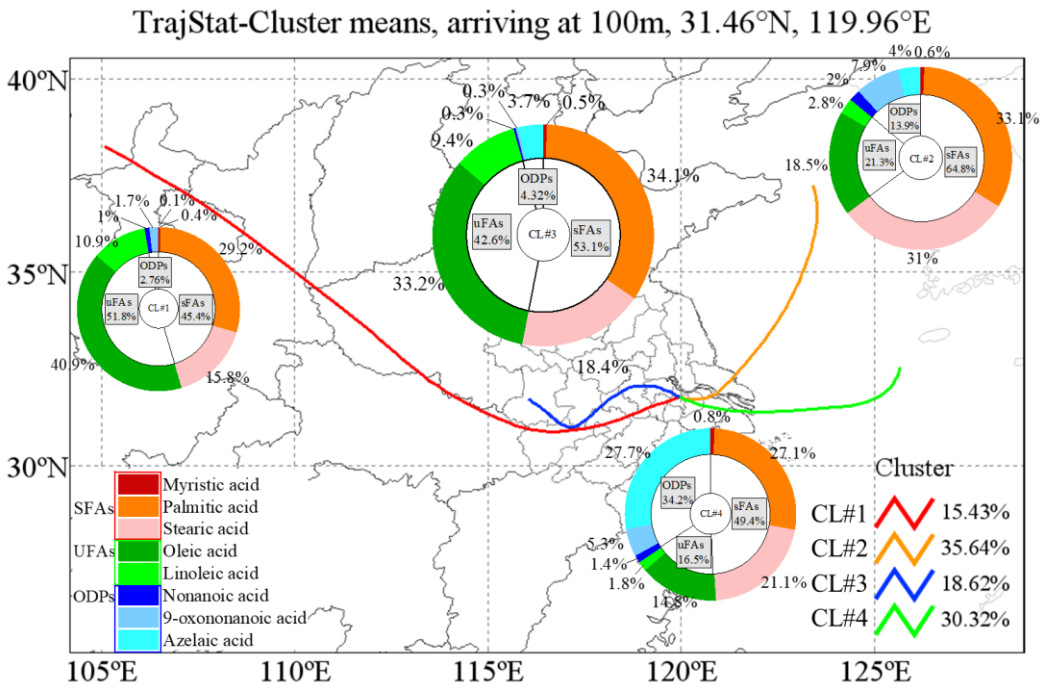

Figure 6. Sources for each air mass during the sampling period. The colored lines in the map show the contribution of each directional air mass source to the total trajectory as resolved by the TrajStat model.

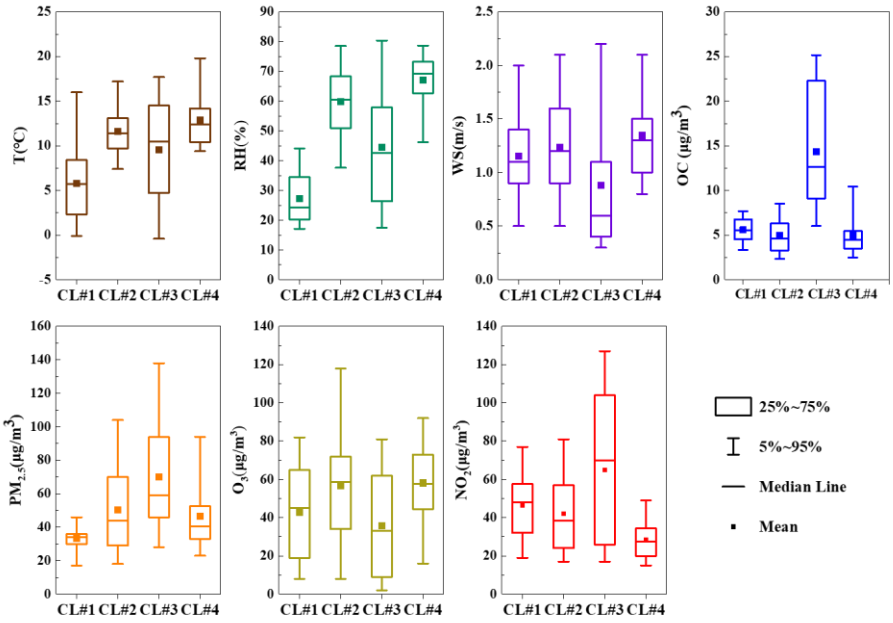

Figure 7. Box plots of meteorological parameters and pollutant concentrations in each cluster (squares and solid lines correspond to the mean and median, respectively; boxes indicate the 25th and 75th percentiles, whiskers are the 5th and 95th percentiles).

3.3 Atmospheric aging of cooking markers

Fig.8(a) shows the diurnal variation of ozone, oleic acid, and ODPs. The ozone concentration started to rise in the morning (06:00) and peaked in the late afternoon (14:00). The diurnal trend of oleic acid was opposite to that of ozone. The diurnal trend of ODPs was also different from oleic acid, the small peak of ODPs was found at around 12:00 in the daytime, which was earlier than that of ozone. At the same time, oxidative decomposition caused significant decrease in the concentration of oleic acid until the dinner time when large amounts of fresh emissions enter the atmosphere again. The decreasing rate of oleic acid concentration slowed down around noon, probably because of fresh cooking emission at lunch time. The diurnal variations of the two products of ozone decomposition of oleic acid (Nonanoic acid and 9-oxononanoic acid) were similar and both peaked around noon, while the production of 9-oxononanoic acid and azelaic acid are in competition (Thornberry and Abbatt, 2004). However, the concentration of 9-oxononanoic acid was significantly higher than that of nonanoic acid (Fig.8, c and d), which may be due to the following reasons: (1) 9-oxononanoic acid can be produced by two pathways, while nonanoic acid generation can only be produced through one of the pathways competing with nonanal, and the molarity generated from the ozonolysis of oleic acid is smaller than that of 9-oxononanoic acid (Gross et al., 2009); (2) due to the high volatility of nonanoic acid, its concentration in the particle phase is much lower, and only a small portion of nonanoic acid in PM is detected by TAG (Wang and Yu, 2021).

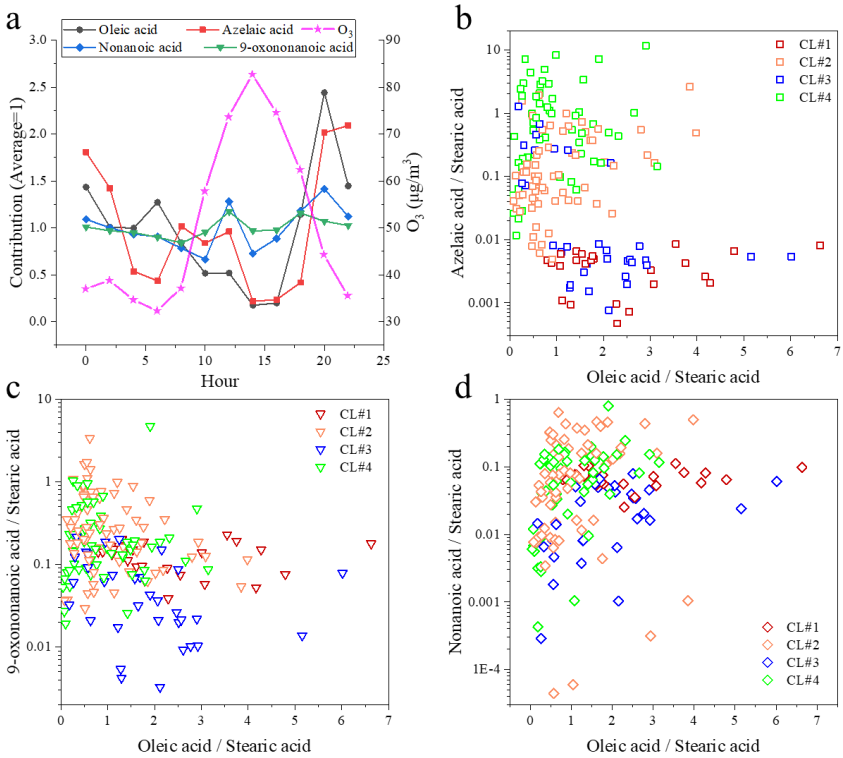

Figure 8. Diurnal variation of C9 products and oleic acid in environmental samples compared to O_3 (a); Correlation of C9 products azelaic acid (b), 9-oxononanoic acid (c), and nonanoic acid (d) with oleic acid.

Fig.8(b) to (d) show the relationship between ODPs / stearic acid ratio and oleic acid/stearic acid. In CL#2 and CL#4, 9-oxononanoic acid / stearic acid ratio is larger than that in CL#1 and CL#3, and azelaic acid /stearic acid ratio have the same characteristic. The nonanoic acid / stearic acid ratio is not well characterized, probably because most of the nonanoic acid is present in the gas phase. Bikkina et al. (2019) found that the O/S ratio exhibited a nonlinear (power) inverse relationship with azelaic acid in remote marine aerosols. This feature was not found in this study, which is possibly due to the single source class of fatty acids and ODPs in remote marine areas, the diversity of emission sources in urban areas, and their vulnerability to transport.

3.4 Oxidative decomposition of uFAs

From the above analysis, cooking emission was the most important source of fatty acids in atmospheric $PM_{2.5}$ in urban areas of Changzhou, especially during the dinner period. Both sFAs and uFAs peaked between 18:00 and 22:00 pm, and then declined until breakfast time in the next day. Fatty acid-like substances in fresh cooking emissions react with various oxidants while being continuously replenished by the fresh cooking emission during the day so that the degradation of uFAs in the particulate phase can be complicated. With no obvious fresh cooking emissions after dinner, and the low volatility of the target pollutants studied (oleic and linoleic acids), the effect of gas-particle partitioning on them can be disregarded, and the evening provides a good opportunity to study the chemical degradation of uFAs from cooking

emissions. Therefore, we selected the period from 18:00 in the evening to 6:00 in the morning, focusing on the impact of oxidants in the atmospheric environment on uFAs. The definition of the effective rate constant k has been described in previous studies (Donahue et al., 2005; Wang and Yu, 2021). To calculate the rate constant of uFAs with oxidants (especially O_3 and NO_3^*, etc), a one-step model was utilized, and an average decay rate constant in each night could be derived. The same method has been used in the study of Wang and Yu (2021), which shows that more than 77% of the observed data fits better with a one-step model. Figures S5 and S6 show the night-time oxidative degradation of oleic acid and linoleic acid, respectively. It should be noted that not all of the reactants (uFAs) will be fully consumed from the start of the fit until fresh emissions enter the atmosphere, and the amount of consumed and remaining uFAs could be affected by a combination of oxidant level, source activity, and meteorological conditions.

Fig.9 shows the effective rate constants of the oxidative decomposition of oleic (k_O) and linoleic (k_L) acids in relation to air oxidants (O_3, NO_2, O_x and NO_3^*, etc. O_x is the total oxidant, calculated from $O_x = NO_2 + O_3$.). It should be noted that the NO_3^*, calculated by multiplying O_3 by NO_2, is a substitution for NO_3^* radical, which is not available in this campaign. Both k_O and k_L had a significant positive correlation (The P values of significance tests were all less than 0.05) with O_3, and no correlation was observed with other air oxidants (O_x, NO_3^* and NO_2). Ozone acted as the predominant oxidant for the oxidative decomposition of uFAs, which was consistent with the conclusion in Shanghai. In addition to the oxidants mentioned above, laboratory studies has also reported N_2O_5 reacts with olefinic acids containing C=C bonds such as oleic acid and linoleic acid, which has a much slower reaction kinetics than that of NO_3^* (Gross et al., 2009). Therefore, the effect of N_2O_5 was ignored in this study.

Fig.10 shows the scatter plot of the effective rate constants of oleic and linoleic acid. The significant correlation between the effective rate constants of oleic acid and linoleic acid was not equal to 1 due to the differences in aerosol composition and environmental conditions. The effective rate constant of oleic acid ranged from 0.08-0.57 h^{-1}, which was overall smaller than k_L (0.16-0.80 h^{-1}), indicating that their reactivity is closely related to their chemical structure, and the two -C=C- bonds in the linoleic make a higher probability in reacting with atmospheric oxidants. However, besides the chemical structure, other factors (e.g., diffusion, and temperature) also affect the calculation of oxidation reaction rate of uFAs. The fitted ratio of k_L/k_O is 1.29 (red dashed line in Fig.11), with most scatters fall in the area with k_L to k_O values above the 1:1. k_L/k_O has a mean value of 1.6 ± 0.3 and the relative reactivity of linoleic acid to oleic acid is below 2 in the measured environmental data, but close to the results of laboratory studies with O_3 as oxidant. We also reviewed the k_L/k_O ratios of O_3, NO_3^* and N_2O_5 as oxidants in other laboratory studies, and the k_L/k_O ratios of the three oxidants were 1.7, 1.8

and 2.9 (Gross et al., 2009; Thornberry and Abbatt, 2004), respectively. The relative reaction coefficients k_I/k_O measured for O_3 in laboratory studies are close to our results. The comparison indicates that O_3 was the most likely oxidants for the nighttime uFAs oxidation in the urban area of Changzhou.

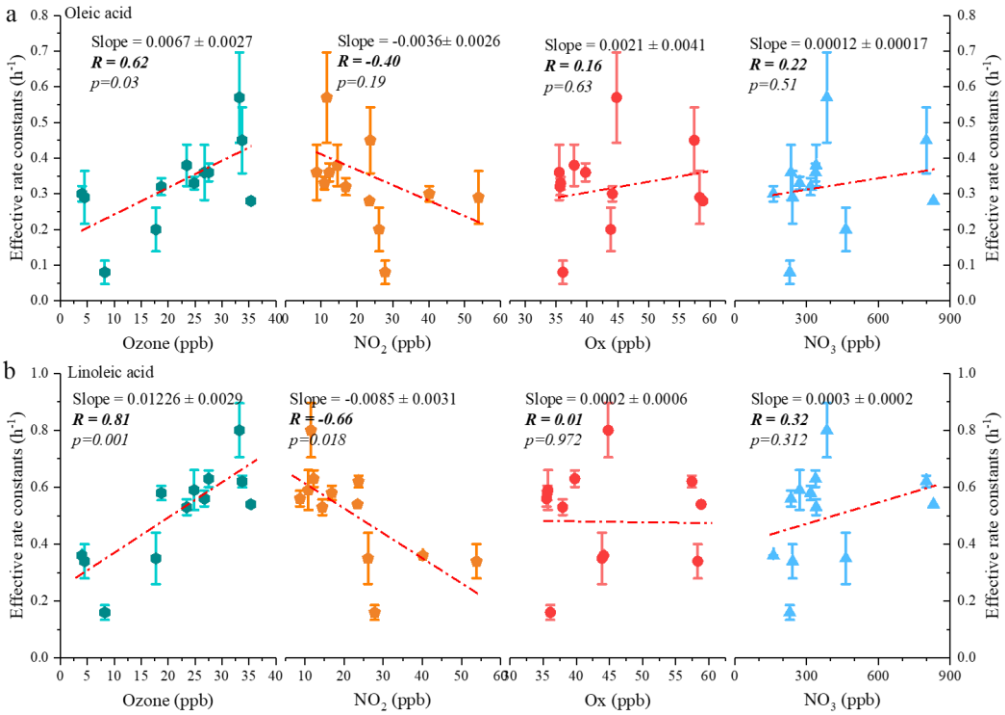

Figure 9. Correlations of the estimated effective decay rate constant with average night-time atmospheric oxidants concentration for oleic acid (a) and linoleic acid (b). (The p-value indicates the parameter of the F-test of the regression equation in the regression model.)

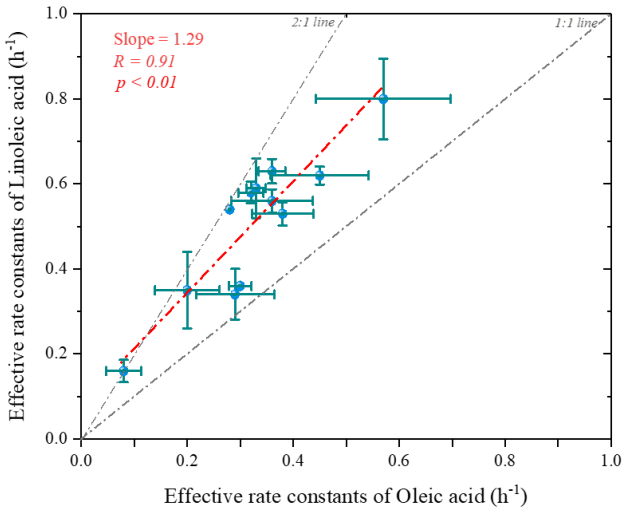

Figure 10. Scatter plot of the estimated effective rate constant for linoleic acid versus oleic acid (The p-value indicates the parameter of the F-test of the regression equation in the regression model).

3.5 Source contributions of cooking aerosol to $PM_{2.5}$ and OC

To gain a more quantitative assessment of source contribution from cooking to OA, PMF was applied for source apportionment. The target POA markers were incorporated into the input data matrix, along with SOA markers (Table S1) and major aerosol components including major ions, elements, EC, and OC. Source apportionment of $PM_{2.5}$ in this field campaign yielded 10 sources, including three secondary sources (secondary sulfate, secondary nitrate and SOA, respectively) and seven primary emission sources (cooking, biomass burning, coal combustion, vehicle exhaust, industrial emissions, dust and fire working, respectively). A detailed description of the identification of each PMF-resolved source factor is shown in section S2. Briefly, secondary source factors account for the largest share of $PM_{2.5}$ (the total was 56.9%, of which secondary nitrate contributes up to 34.4%), and primary emissions contributed to 43.1% of total $PM_{2.5}$ (Fig.11). Among the primary source factors, industry makes the largest contribution to $PM_{2.5}$ mass concentration (9.9%).

In a specific pollution period, different sources have different impacts on $PM_{2.5}$ concentration and chemical compositions in Changzhou. Among the 10 sources, the cooking factor was dominated by sFAs and uFAs during the monitoring period, accounting for 4.6% of the total $PM_{2.5}$. The concentration of cooking source and its contribution to total $PM_{2.5}$ also showed a clear diurnal variation, with two peaks at around 6:00 and 20:00, respectively, especially at the dinner time. The contribution of cooking to $PM_{2.5}$ concentration during mealtime increased significantly compared with other periods, reaching 7.8% at dinner time. The mean concentration of cooking aerosol in the polluted period was estimated to be 4.0 $\mu g/m^3$, which was 5.3 times higher than that in the clean period (0.75 $\mu g/m^3$). The variation was similar to that of fatty acids. The factor profiles of the 10-factor constrained run of PMF are shown in section S2 and Figure S5, together with the time series of contributions from individual source factors. Overall, we estimated that cooking accounted for 5.8% of the total $PM_{2.5}$ during the pollution period, which was 1.9 times greater than that of 3.0% during the clean period. During the whole observation period, the cooking factor contributes only a small part of $PM_{2.5}$, but it accounts for 8.1% of the total OC, indicating the importance of cooking emissions to organic matter, which is a significant source of organic pollution in urban areas.

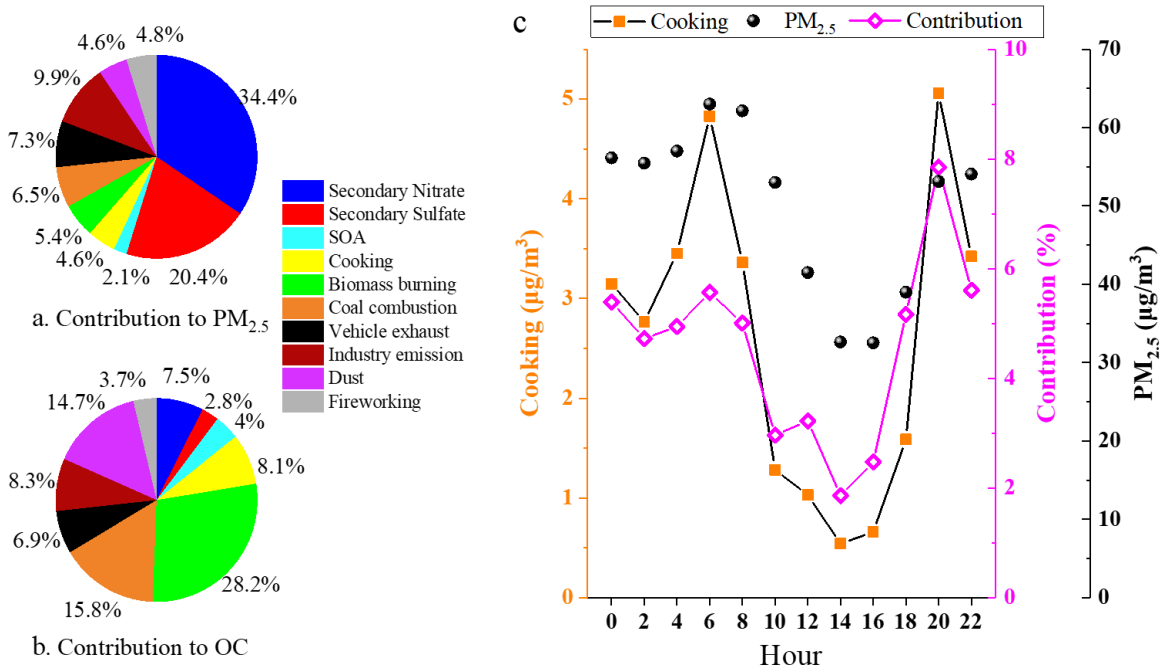

Figure 11. Comparison of individual factor contributions to $PM_{2.5}$ (a) and OC (b); diurnal variation of cooking source (c).

4. Conclusions

In this study, we measured uFAs, sFAs, and ODPs every two hours using TAG in the urban Changzhou city. The concentration of TFAs averaged at 105.70 ng/m^3, close to that in Shanghai. The average concentration of TFAs in polluted period was 147.06 ng/m^3, which was 4.2 times higher than that during clean period. During the rising period of $PM_{2.5}$, TFAs concentration tends to reach the peak earlier than $PM_{2.5}$, and the proportion of TFAs in $PM_{2.5}$ as well as OC will increase first and then decrease. However, when affected by adverse diffusion, TFAs concentration will accumulate continuously as $PM_{2.5}$.

Fatty acid concentration showed a clear diurnal variation, peaking at 6:00 am in the morning and 20:00 pm around dinner time. The average contribution of cooking to $PM_{2.5}$ was estimated to be 4.6%, while the contribution to total OC reached 8.1%. However, the proportion of cooking to total $PM_{2.5}$ among different sources during the meal period increased significantly compared with other periods, especially during the dinner period, peaking at 7.8%. The linoleic acid /stearic acid and oleic acid /stearic acid ratios exhibited a significant peak during dinnertime, which was close to the cooking source profile values, and a relatively smaller peak at lunchtime. Cooking sources during dinner hours are the most important contributors to the concentration of fatty acids in $PM_{2.5}$ during the study period. Diurnal trend of ODPs was different from that of uFAs, and the concentration of ODPs increased significantly at noon. The diurnal variations of nonanoic acid and 9-oxononanoic acid in ODPs are similar, mainly because oleic acid can produce both 9-oxononanoic acid and nonanoic acid in the ozonolysis pathway.

Under the influence of different air masses, there were significant variations in the ratios of various organic acids from cooking. Highest total concentrations of sFAs, uFAs and ODPs were found under the local air mass cluster (CL#3), indicating significant local emissions contributing to fatty acids as well as $PM_{2.5}$. And the percentages of TFAs in CL#1 and CL#3 were larger than that in CL#2 and CL#4. The proportion of ODPs in CL#2 and CL#4 was greater than that in CL#1 and CL#3. This is mainly because under the influence of transportation, the air masses brought more sFAs, ODPs. The air masses were more aged, and the higher ozone concentration and more active uFAs decomposition reaction occurred in these two air mass clusters. The daily oxidative degradation kinetics of oleic and linoleic acids were obtained using data during nighttime of each observation date. The k_O ranged from 0.08 to 0.57 h^{-1}, which was overall smaller than k_L (0.16-0.80 h^{-1}). It was observed that both k_O and k_L had a significant positive correlation with O_3. The relative reaction coefficients k_L/k_O (1.6 ±0.3) of linoleic and oleic acids in this study are close to k_L/k_O measured for O_3 in laboratory studies, indicating that O_3 was the main nighttime oxidants for uFAs in Changzhou City. Overall, this study describes the concentration variation and oxidative degradation of uFAs and oxidation products in ambient air based on hourly time-resolved observations, guiding future refinement of source apportionment of $PM_{2.5}$ and the development of cooking emission control policies. The contribution of cooking aerosol to $PM_{2.5}$ is 4.6% on average, rising to 7.8% at dinner time, and the fatty acid concentration as cooking tracers increased significantly during dinner time compared with afternoon. It is estimated that cooking source accounted for 5.8% of the total $PM_{2.5}$ during the pollution period, which was 1.9 times greater than the 3.0% during the clean period, showing that strict control on cooking emissions should be paid more attention during pollution episodes.

ACKNOWLEDGEMENTS

This study is financially supported by the National Natural Science Foundation of China (NO. 41875161, 42075144 and 42005112). We thank Changzhou Environmental Monitoring Center of Jiangsu Province to help conduct the field campaign.

AUTHOR CONTRIBUTIONS

RL, KZ, QL and LMY conducted the field measurements. RL and KZ performed the data analysis and prepared the manuscript with contributions from all co-authors. LL formulated the research goals and edited and reviewed the manuscript. LL and JZY reviewed and edited the manuscript. All authors contributed to data interpretations and discussions.

COMPETING INTERESTS

The authors declare no conflict of interest.

DATA AND CODE AVAILABILITY

This paper does not report original code. Data is available from the corresponding author (Lily@shu.edu.cn) upon request.

REFERENCES

Amato, F., Pandolfi, M., Escrig, A., Querol, X., Alastuey, A., Pey, J., Perez, N., and Hopke, P. K.: Quantifying road dust resuspension in urban environment by Multilinear Engine: A comparison with PMF2, Atmos. Environ., 43(17), 2770-2780, doi:10.1016/j.atmosenv.2009.02.039, 2009.

Bertrand, A., Stefenelli, G., Jen, C. N., Pieber, S. M., Bruns, E. A., Ni, H. Y., Temime-Roussel, B., Slowik, J. G., Goldstein, A. H., El Haddad, I., Baltensperger, U., Prevot, A. S. H., Wortham, H., and Marchand, N.: Evolution of the chemical fingerprint of biomass burning organic aerosol during aging, Atmos Chem Phys, 18(10), 7607-7624, doi:10.5194/acp-18-7607-2018, 2018a.

Bertrand, A., Stefenelli, G., Pieber, S. M., Bruns, E. A., Temime-Roussel, B., Slowik, J. G., Wortham, H., Prevot, A. S. H., El Haddad, I., and Marchand, N.: Influence of the vapor wall loss on the degradation rate constants in chamber experiments of levoglucosan and other biomass burning markers, Atmos Chem Phys, 18(15), 10915-10930, doi:10.5194/acp-18-10915-2018, 2018b.

Bikkin, P., Kawamura, K., Bikkina, S., Kunwar, B., Tanaka, K., and Suzuki, K.: Hydroxy Fatty Acids in Remote Marine Aerosols over the Pacific Ocean: Impact of Biological Activity and Wind Speed, Acs Earth Space Chem, 3(3), 366-379, doi:10.1021/acsearthspacechem.8b00161, 2019.

Cai, T. Q., Zhang, Y., Fang, D. Q., Shang, J., Zhang, Y. X., and Zhang, Y. H.: Chinese vehicle emissions characteristic testing with small sample size: Results and comparison, Atmos Pollut Res, 8(1), 154-163, doi:10.1016/j.apr.2016.08.007, 2017.

Donahue, N. M., Robinson, A. L., Huff Hartz, K. E., Sage, A. M., and Weitkamp, E. A.: Competitive oxidation in atmospheric aerosols: The case for relative kinetics, Geophys. Res. Lett., 32(16), doi:10.1029/2005gl022893, 2005.

Fortenberry, C., Walker, M., Dang, A., Loka, A., Date, G., de Caryalho, K. C., Morrison, G., and Williams, B.: Analysis of indoor particles and gases and their evolution with natural ventilation, Indoor Air, 29(5), 761-779, doi:10.1111/ina.12584, 2019.

Gross, S., Iannone, R., Xiao, S., and Bertram, A. K.: Reactive uptake studies of NO_3 and N_2O_5 on alkenoic acid, alkanoate, and polyalcohol substrates to probe nighttime aerosol chemistry, PCCP, 11(36), 7792-7803, doi:10.1039/b904741g, 2009.

Hays, M. D., Geron, C. D., Linna, K. J., Smith, N. D., and Schauer, J. J.: Speciation of gas-phase and fine particle emissions from burning of foliar fuels, Environmental Science & Technology, 36(11), 2281-2295, doi:10.1021/es0111683, 2002.

He, L. Y., Hu, M., Huang, X. F., Yu, B. D., Zhang, Y. H., and Liu, D. Q.: Measurement of emissions of fine particulate organic matter from Chinese cooking, Atmos. Environ., 38(38), 6557-6564, doi:10.1016/j.atmosenv.2004.08.034, 2004.

Ho, K. F., Huang, R. J., Kawamura, K., Tachibana, E., Lee, S. C., Ho, S. S. H., Zhu, T., and Tian, L.: Dicarboxylic acids, ketocarboxylic acids, alpha-dicarbonyls, fatty acids and benzoic acid in $PM_{2.5}$ aerosol collected during CAREBeijing-2007: an effect of traffic restriction on air quality, Atmos Chem Phys, 15(6), 3111-3123, doi:10.5194/acp-15-3111-2015, 2015.

Hou, X. M., Zhuang, G. S., Sun, Y., and An, Z. S.: Characteristics and sources of polycyclic aromatic hydrocarbons and fatty acids in $PM_{2.5}$ aerosols in dust season in China, Atmos. Environ., 40(18), 3251-3262,

doi:10.1016/j.atmosenv.2006.02.003, 2006.

Huang, D. D., Zhu, S. H., An, J. Y., Wang, Q. Q., Qiao, L. P., Zhou, M., He, X., Ma, Y. G., Sun, Y. L., Huang, C., Yu, J. Z., and Zhang, Q.: Comparative Assessment of Cooking Emission Contributions to Urban Organic Aerosol Using Online Molecular Tracers and Aerosol Mass Spectrometry Measurements, Environmental Science & Technology, 55(21), 14526-14535, doi:10.1021/acs.est.1c03280, 2021.

Huang, X. Q., Han, D. M., Cheng, J. P., Chen, X. J., Zhou, Y., Liao, H. X., Dong, W., and Yuan, C.: Characteristics and health risk assessment of volatile organic compounds (VOCs) in restaurants in Shanghai, Environ Sci Pollut R, 27(1), 490-499, doi:10.1007/s11356-019-06881-6, 2020.

Kanakidou, M., Seinfeld, J. H., Pandis, S. N., Barnes, I., Dentener, F. J., Facchini, M. C., Van Dingenen, R., Ervens, B., Nenes, A., Nielsen, C. J., Swietlicki, E., Putaud, J. P., Balkanski, Y., Fuzzi, S., Horth, J., Moortgat, G. K., Winterhalter, R., Myhre, C. E. L., Tsigaridis, K., Vignati, E., Stephanou, E. G., and Wilson, J.: Organic aerosol and global climate modelling: a review, Atmos Chem Phys, 5, 1053-1123, doi:10.5194/acp-5-1053-2005, 2005.

Lee, S., Liu, W., Wang, Y. H., Russell, A. G., and Edgerton, E. S.: Source apportionment of $PM_{2.5}$: Comparing PMF and CMB results for four ambient monitoriniz sites in the southeastern United States, Atmos. Environ., 42(18), 4126-4137, doi:10.1016/j.atmosenv.2008.01.025, 2008.

Li, L., Wu, D., Chang, X., Tang, Y., Hua, Y., Xu, Q. C., Deng, S. H., Wang, S. X., and Hao, J. M.: Polar organic aerosol tracers in two areas in Beijing-Tianjin-Hebei region: Concentration comparison before and in the sept. Third Parade and sources, Environ. Pollut., 270, doi:10.1016/j.envpol.2020.116108, 2021.

Li, R., Wang, Q. Q., He, X., Zhu, S. H., Zhang, K., Duan, Y. S., Fu, Q. Y., Qiao, L. P., Wang, Y. J., Huang, L., Li, L., and Yu, J. Z.: Source apportionment of $PM_{2.5}$ in Shanghai based on hourly organic molecular markers and other source tracers, Atmos Chem Phys, 20(20), 12047-12061, doi:10.5194/acp-20-12047-2020, 2020.

Nah, T., Kessler, S. H., Daumit, K. E., Kroll, J. H., Leone, S. R., and Wilson, K. R.: Influence of Molecular Structure and Chemical Functionality on the Heterogeneous OH-Initiated Oxidation of Unsaturated Organic Particles, J. Phys. Chem. A, 118(23), 4106-4119, doi:10.1021/jp502666g, 2014.

Norris, G., Duvall, R., Brown, S., and Bai, S.: EPA Positive Matrix Factorization (PMF) 5.0 Fundamentals and User Guide, 2014.

Oliveira, C., Pio, C., Alves, C., Evtyugina, M., Santos, P., Goncalves, V., Nunes, T., Silvestre, A. J. D., Palmgren, F., Wahlin, P., and Harrad, S.: Seasonal distribution of polar organic compounds in the urban atmosphere of two large cities from the North and South of Europe, Atmos. Environ., 41(27), 5555-5570, doi:10.1016/j.atmosenv.2007.03.001, 2007.

Pei, B., Cui, H. Y., Liu, H., and Yan, N. Q.: Chemical characteristics of fine particulate matter emitted from commercial cooking, Front Env Sci Eng, 10(3), 559-568, doi:10.1007/s11783-016-0829-y, 2016.

Pleik, S., Spengler, B., Schafer, T., Urbach, D., Luhn, S., and Kirsch, D.: Fatty Acid Structure and Degradation Analysis in Fingerprint Residues, J. Am. Soc. Mass. Spectrom., 27(9), 1565-1574, doi:10.1007/s13361-016-1429-6, 2016.

Ren, H. X., Xue, M., An, Z. J., Zhou, W., and Jiang, J. K.: Quartz filter-based thermal desorption gas chromatography mass spectrometry for in-situ molecular level measurement of ambient organic aerosols, J. Chromatogr. A, 1589, 141-148, doi:10.1016/j.chroma.2019.01.010, 2019.

Ringuet, J., Leoz-Garziandia, E., Budzinski, H., Villenave, E., and Albinet, A.: Particle size distribution of nitrated and oxygenated polycyclic aromatic hydrocarbons (NPAHs and OPAHs) on traffic and suburban sites of a European megacity: Paris (France), Atmos Chem Phys, 12(18), 8877-8887, doi:10.5194/acp-12-8877-2012, 2012.

Rogge, W. F., Hildemann, L. M., Mazurek, M. A., Cass, G. R., and Simoneit, B.: Sources of fine organic aerosol. 4. Particulate abrasion products from leaf surfaces of urban plants, Environmental Science & Technology, 27(13), 2700-2711, 1993.

Rogge, W. F., Medeiros, P. M., and Simoneit, B. R. T.: Organic marker compounds for surface soil and fugitive dust from open lot dairies and cattle feedlots, Atmos. Environ., 40(1), 27-49, doi:10.1016/j.atmosenv.2005.07.076, 2006.

Schauer, C., Niessner, R., and Poschl, U.: Polycyclic aromatic hydrocarbons in urban air particulate matter: Decadal and seasonal trends, chemical degradation, and sampling artifacts, Environmental Science & Technology, 37(13), 2861-2868, doi:10.1021/es034059s, 2003.

Schauer, J. J., Kleeman, M. J., Cass, G. R., and Simoneit, B. R. T.: Measurement of emissions from air pollution sources. 3. C-1-C-29 organic compounds from fireplace combustion of wood, Environmental Science & Technology, 35(9), 1716-1728, doi:10.1021/es001331e, 2001.

Schauer, J. J., Kleeman, M. J., Cass, G. R., and Simoneit, B. R. T.: Measurement of emissions from air pollution sources. 4. C-1-C-27 organic compounds from cooking with seed oils, Environmental Science & Technology, 36(4), 567-575, doi:10.1021/es002053m, 2002.

Simoneit, B. R. T.: Biomass burning - A review of organic tracers for smoke from incomplete combustion, Appl. Geochem., 17(3), 129-162, doi:10.1016/S0883-2927(01)00061-0, 2002.

Thornberry, T., and Abbatt, J. P. D.: Heterogeneous reaction of ozone with liquid unsaturated fatty acids: detailed kinetics and gas-phase product studies, PCCP, 6(1), 84-93, doi:10.1039/b310149e, 2004.

Vesna, O., Sax, M., Kalberer, M., Gaschen, A., and Ammann, M.: Product study of oleic acid ozonolysis as function of humidity, Atmos. Environ., 43(24), 3662-3669, doi:10.1016/j.atmosenv.2009.04.047, 2009.

Wang, Q., Shao, M., Zhang, Y., Wei, Y., Hu, M., and Guo, S.: Source apportionment of fine organic aerosols in Beijing, Atmos Chem Phys, 9(21), 8573-8585, doi:10.5194/acp-9-8573-2009, 2009.

Wang, Q. Q., He, X., Huang, X. H. H., Griffith, S. M., Feng, Y. M., Zhang, T., Zhang, Q. Y., Wu, D., and Yu, J. Z.: Impact of Secondary Organic Aerosol Tracers on Tracer-Based Source Apportionment of Organic Carbon and $PM_{2.5}$: A Case Study in the Pearl River Delta, China, Acs Earth Space Chem, 1(9), 562-571, doi:10.1021/acsearthspacechem.7b00088, 2017.

Wang, Q. Q., He, X., Zhou, M., Huang, D. D., Qiao, L. P., Zhu, S. H., Ma, Y. G., Wang, H. L., Li, L., Huang, C., Huang, X. H. H., Xu, W., Worsnop, D., Goldstein, A. H., Guo, H., and Yu, J. Z.: Hourly Measurements of Organic Molecular Markers in Urban Shanghai, China: Primary Organic Aerosol Source Identification and Observation of Cooking Aerosol Aging, Acs Earth Space Chem, 4(9), 1670-1685, doi:10.1021/acsearthspacechem.0c00205, 2020.

Wang, Q. Q., and Yu, J. Z.: Ambient Measurements of Heterogeneous Ozone Oxidation Rates of Oleic, Elaidic, and Linoleic Acid Using a Relative Rate Constant Approach in an Urban Environment, Geophys. Res. Lett., 48(19), doi:10.1029/2021GL095130, 2021.

Yee, L. D., Isaacman-VanWertz, G., Wernis, R. A., Meng, M., Rivera, V., Kreisberg, N. M., Hering, S. V., Bering, M. S., Glasius, M., Upshur, M. A., Be, A. G., Thomson, R. J., Geiger, F. M., Offenberg, J. H., Lewandowski, M., Kourtchev, I., Kalberer, M., de Sa, S., Martin, S. T., Alexander, M. L., Palm, B. B., Hu, W. W., Campuzano-Jost, P., Day, D. A., Jimenez, J. L., Liu, Y. J., McKinney, K. A., Artaxo, P., Viegas, J., Manzi, A., Oliveira, M. B., de Souza, R., Machado, L. A. T., Longo, K., and Goldstein, A. H.: Observations of sesquiterpenes and their oxidation products in central Amazonia during the wet and dry seasons, Atmos Chem Phys, 18(14), 10433-10457, doi:10.5194/acp-18-10433-2018, 2018.

Zahardis, J., and Petrucci, G. A.: The oleic acid-ozone heterogeneous reaction system: products, kinetics, secondary chemistry, and atmospheric implications of a model system - a review, Atmos Chem Phys, 7, 1237-1274, doi:10.5194/acp-7-1237-2007, 2007.

Zhang, K., Yang, L. M., Li, Q., Li, R., Zhang, D. P., Xu, W., Feng, J. L., Wang, Q. Q., Wang, W., Huang, L., Yaluk, E. A., Wang, Y. J., Yu, J. Z., and Li, L.: Hourly measurement of $PM_{2.5}$-bound nonpolar organic compounds in Shanghai: Characteristics, sources and health risk assessment, Sci. Total Environ., 789, doi:10.1016/j.scitotenv.2021.148070, 2021.

Zhang, N., Han, B., He, F., Xu, J., Zhao, R. J., Zhang, Y. J., and Bai, Z. P.: Chemical characteristic of $PM_{2.5}$ emission and inhalational carcinogenic risk of domestic Chinese cooking, Environ. Pollut., 227, 24-30, doi:10.1016/j.envpol.2017.04.033, 2017.

Zhang, Y. X., Schauer, J. J., Zhang, Y. H., Zeng, L. M., Wei, Y. J., Liu, Y., and Shao, M.: Characteristics of particulate carbon emissions from real-world Chinese coal combustion, Environmental Science & Technology, 42(14), 5068-5073, doi:10.1021/es7022576, 2008.

Zhang, Y. X., Shao, M., Zhang, Y. H., Zeng, L. M., He, L. Y., Zhu, B., Wei, Y. J., and Zhu, X. L.: Source profiles of particulate organic matters emitted from cereal straw burnings, J Environ Sci, 19(2), 167-175, doi:10.1016/S1001-0742(07)60027-8, 2007.

Zhao, X. Y., Hu, Q. H., Wang, X. M., Ding, X., He, Q. F., Zhang, Z., Shen, R. Q., Lu, S. J., Liu, T. Y., Fu, X. X., and Chen, L. G.: Composition profiles of organic aerosols from Chinese residential cooking: case study in urban Guangzhou, south China, J Atmos Chem, 72(1), 1-18, doi:10.1007/s10874-015-9298-0, 2015.

Zhao, Y. L., Hu, M., Slanina, S., and Zhang, Y. H.: Chemical compositions of fine particulate organic matter emitted from Chinese cooking, Environmental Science & Technology, 41(1), 99-105, doi:10.1021/es0614518, 2007.

Ziemann, P. J.: Aerosol products, mechanisms, and kinetics of heterogeneous reactions of ozone with oleic acid in pure and mixed particles, Faraday Discuss., 130, 469-490, doi:10.1039/b417502f, 2005.